EurJOC
European Journal of Organic Chemistry

Research Article
doi.org/10.1002/ejoc.202101521

Chemistry Europe
European Chemical Societies Publishing

www.eurjoc.org

Special Collection

Annelated Pyridine Bases for the Selective Acylation of 1,2-Diols

Stefanie Mayr[a] and Hendrik Zipse*[a]

In memory of Klaus Hafner

A set of 24 annelated derivatives of 4-diaminopyridine (DMAP) has been synthesized and tested with respect to its catalytic potential in the regioselective acylation of 1,2-diol substrates. The Lewis basicities of the catalysts as quantified through quantum chemical calculations vary due to inductive substituent effects and intramolecular stacking interactions between side chain π-systems and the pyridinium core ring system. The primary over secondary hydroxyl group selectivities in catalytic acylations of 1,2-diol substrates depend on the size and the steric demand of the Lewis base and the anhydride reagent.

Introduction

The protection of functional groups plays an important role in organic synthesis.[1] In most natural products such as sugars or pharmaceutically important molecules, hydroxyl groups are present in large numbers,[2] and the selective protection and deprotection of these groups is thus highly relevant in organic chemistry.[3] The highly chemo- and regioselective transformation of hydroxyl groups in polyol systems provides particular challenges, despite the considerable attention this area has seen already in the last decades.[4] One of the most prominent ways to protect alcohols is the Lewis base-mediated esterification using a variety of acylation reagents such as acid chlorides, cyanides or acid anhydrides.[5] Aside from organocatalyst classes such as isothioureas,[6,7a] phosphanes,[7] amidines,[7a,e] or *N*-alkylimidazols,[7a,f] pyridine-based catalysts like 4-dimethylaminopyridine (DMAP, **1**) count among the most often used Lewis base catalysts for these transformations.[5f,7a,8,9] The catalytic activity of **1** can be increased through installation of stronger electron donors at the C4 position as is, for example, the case in 4-(pyrrolidinyl)pyridine (PPY, **2**).[9a,10] A further improvement in catalytic activity was achieved with tricyclic 4-aminopyridine derivative 9-azajulolidine (TCAP, **3**), where the 4-amino nitrogen atom is conformationally fixed.[11] A mechanistic study by Steglich *et al.*[11] indicated that the stability of the respective acylpyridinium ions correlates strongly with experimentally measured acylation rates. Further extensions of this idea led to the more nucleophilic Lewis bases of the 3,4-diaminopyridine type **4** (R=Ph, Me), which perform quite well in the acylation of tertiary alcohols.[12] For the chiral catalyst **A** employed in kinetic resolution experiments by Fuji *et al.*[13] it was demonstrated by ^{1}H NMR analysis (and later confirmed through quantum chemical studies[14]) that the respective acylpyridinium intermediate is stabilized by cation-π interactions. Combining these concepts one can envision a class of intrinsically electron-rich 3,4-diaminopyridine catalysts for the acylation of alcohols carrying a π-system (or dispersion-energy donor, DED) side chain of general structure **B**. Reaction of **B** with acyl donor **C** will generate the acylpyridinium ion **D** as a key intermediate of the catalytic cycle. If designed properly this latter intermediate will be stabilized through stacking interactions between the side chain substituents and the formally cationic pyridinium core ring system as shown in the "closed" conformation **D** in Scheme 1. Subsequent reaction with alcohol **E** then completes the catalytic sequence. Whether or not the

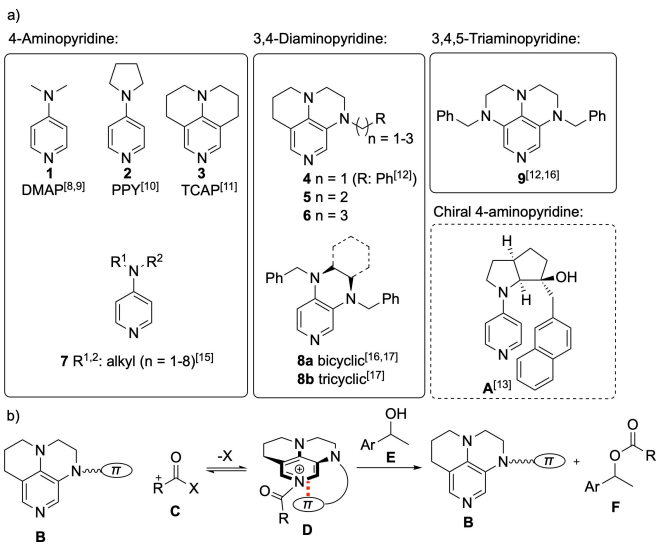

Scheme 1. a) Basic motif of pyridinium Lewis based catalysts. b) Stabilization of *N*-acylpyridinium cation intermediate by non-covalent interactions (NCI).

[a] *S. Mayr, Dr. H. Zipse*
Department of Chemistry
LMU München
Butenandtstr. 5–13, 81366 München, Germany
E-mail: zipse@cup.uni-muenchen.de
www.cup.uni-muenchen.de/oc/zipse/

Supporting information for this article is available on the WWW under https://doi.org/10.1002/ejoc.202101521

Part of the "Special Collection in Memory of Klaus Hafner".

Research Article
doi.org/10.1002/ejoc.202101521

closed conformation of acylpyridinium intermediate **D** actually exists will depend on the type of side chain DED donor as well as the length of the linker connecting these two units. The latter aspect is best seen in catalysts **4**–**6**, where the linker length is systematically increased from n = 1 to n = 3. For catalysts of type **7** it is already known that *n*-alkyl substituents can influence catalytic activity also through inductive effects.[15] This also appears to be a factor in the excellent catalytic performance of 3,4-diaminopyridine catalysts of general structure **8**,[16,17] where derivative **8b** was found to be similarly active as TCAP (**3**) and **4** in many transformations. 3,4,5-Triaminopyridines such as **9** appear to be even stronger Lewis bases as compared to all other compounds shown in Scheme 1, but this basicity increase does not appear to translate into higher catalytic reactivity.[12,16] Although the stereoselectivity of Lewis base-mediated acylation reactions has been studied extensively (and successfully),[5f,7,18] this is much less the case for regioselective acylations in polyol systems. Noteworthy exceptions exist for acylations of carbohydrate substrates, where the use of highly functionalized catalysts based on the PPY substructure[19] and/or the exploitation of specific hydrogen bonding effects with selected counter ions[5a,20] lead to selective acylations of secondary over primary OH groups. We have recently analyzed the influence of anhydride size and substitution pattern on the acylation of secondary alcohol **G** over primary alcohol **H** catalysed by the Lewis base TCAP.[21] Exploiting π-π-interactions between secondary alcohol **G** and the planar TCAP motif as well as size effects of the anhydride reagents, it was indeed possible to steer intermolecular competition reactions towards preferred acylation of the secondary alcohol **G** (Figure 1, left side). The same factors were subsequently also found to impact the *intramolecular* competition between primary and secondary OH groups in 1,2-diols of general structure **I** (Figure 1, right side).[22] In absolute terms the regioselectivity of the TCAP-mediated process was found to be quite moderate in the first acylation step and then to increase in acylations of the initially formed monoesters. In kinetic resolution experiments it was already demonstrated earlier that size effects can have a strong influence on the enantioselectivity.[18,23] In the present study we now probe the influence of catalyst structure on the regioselectivity of diols **I**. More specifically we analyze how the DED substituents in catalysts of general structure **4**–**6** impact regioselectivity and catalytic efficiency. The Lewis basicities of these catalysts have been quantified by quantum mechanically calculated acetyl cation affinity numbers.

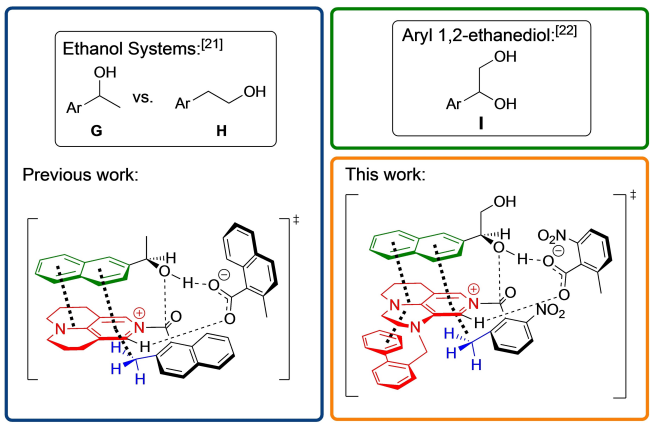

Figure 1. Transition structure for the acylation of 1-(2-naphthyl)ethanol catalysed by TCAP (**3**) (left) and proposed transition structure for the acylation of 1-(2-naphthyl)ethane-1,2-diol catalysed by modified TCAP catalysts **4**–**6** (right).

Results and Discussion

Competition experiments

Catalysts **1**–**6** and **8b**[24] were first characterized with respect to their ability to selectively acylate primary or secondary hydroxyl groups in turnover-limited competition experiments. As a benchmark reaction we select the acylation of secondary 1-(naphth-2-yl)ethanol **10** vs. primary 2-(naphth-2-yl)ethanol **11** to the corresponding esters (Scheme 2).[21,25] The relative rate constant k_{rel} reflecting the selectivities of the formation of the products **12** and **13** is here defined as the ratio between the effective rate constant k_2 for acylation of primary alcohol **11** and the effective rate constant k_1 for acylation of secondary alcohol **10**. As acylation reagent 2-methyl-6-nitrobenzoic anhydride **14** was selected due to its comparatively high reactivity and preference for secondary alcohols identified in earlier studies.[21–22] Turnover-limited competition experiments were performed with a 1:1 mixture of **10** and **11** adding **14** as the limiting acylation reagent to allow conversions of 20–70%, an excess of auxiliary base Et_3N (**15**), and 10 mol% of the corresponding Lewis-base catalysts **1**–**6**,**8b** in $CDCl_3$ at +23 °C. By determining the chemoselectivity at various conversion points, the relative reaction rates can be determined following the analysis method established by Kagan *et al.*[26] for kinetic resolution experiments (for details see SI). Three different classes of tricyclic pyridine-based catalysts were synthesized (Figure 2). The first class **4a**-**r** contains a tricyclic 3,4-diaminopyridine core unit connected via a short CH_2-linker (n = 1) to a selection of small (**4a**–**l**, **4n**,**o** and **4r**) or larger (**4j**–**m**) aromatic and aliphatic (**4p**,**q**) side chains. The effects of longer linker units are explored in class II (n = 2, **5a**–**b**) and class III (n = 3,

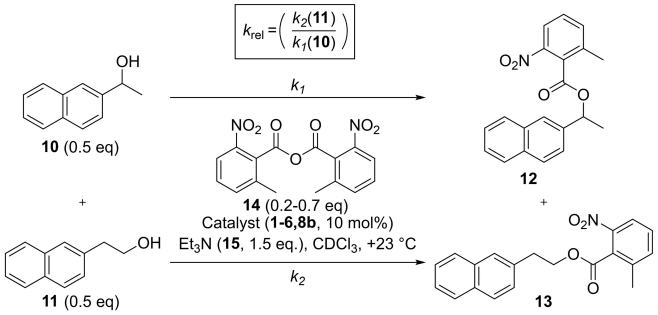

Scheme 2. Turnover-limited competition experiment between alcohols **10** and **11** with anhydride **14** catalysed by Lewis base catalysts **1**–**6** and **8b**.

Research Article
doi.org/10.1002/ejoc.202101521

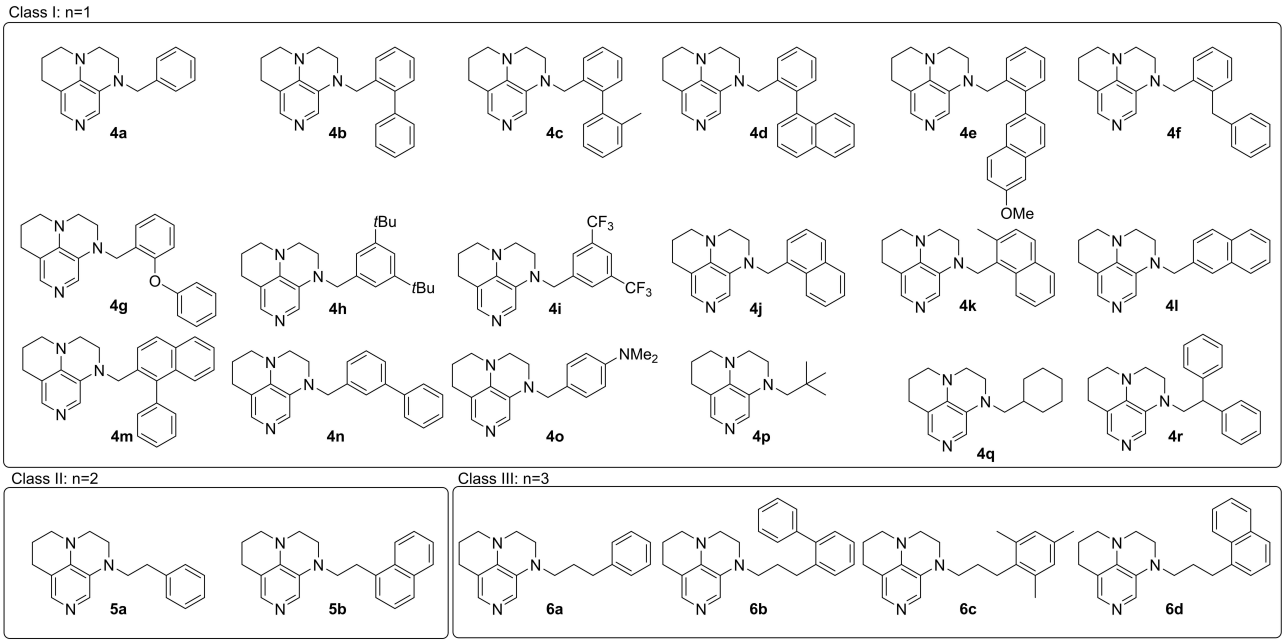

Figure 2. Structures and classifications of catalysts **4**–**6**.

6a–**d**), where the attached aromatic side chains can potentially fold back onto the 3,4-diaminopyridine core unit more easily. For the sake of comparison we also include the established catalysts DMAP (**1**), PPY (**2**), and TCAP (**3**) as well as the tricyclic diaminopyridine derivative **8b.**[12,27]

The acylation of **10** and **11** catalysed with the most common 4-aminopyridine based catalyst DMAP (**1**) is a good reference point with $k_{rel} = 1.44$, which indicates that the primary alcohol **11** reacts 1.4 times as fast as the secondary alcohol **10** (red bar in Figure 3). PPY (**2**) shows a drop in selectivity to $k_{rel} = 1.24$ and thus a reduced preference for primary alcohol **11**. The selectivity value inverts to $k_{rel} = 0.68$ when using the tricyclic 4-aminopyridine TCAP (**3**), which implies that secondary alcohol **10** reacts 1.4 times as fast as primary alcohol **11** (green bar in Figure 3).

In the 3,4-aminopyridine catalysts **4** we first explored the influence of an attached *ortho*-substituted phenyl group. The catalytic reaction with **4a** (R=Ph) shows a selectivity of $k_{rel} = 0.78$. By functionalizing the attached phenyl group in *ortho* position with aryl substituents (such as Ph, Tol, or 1-Np) the

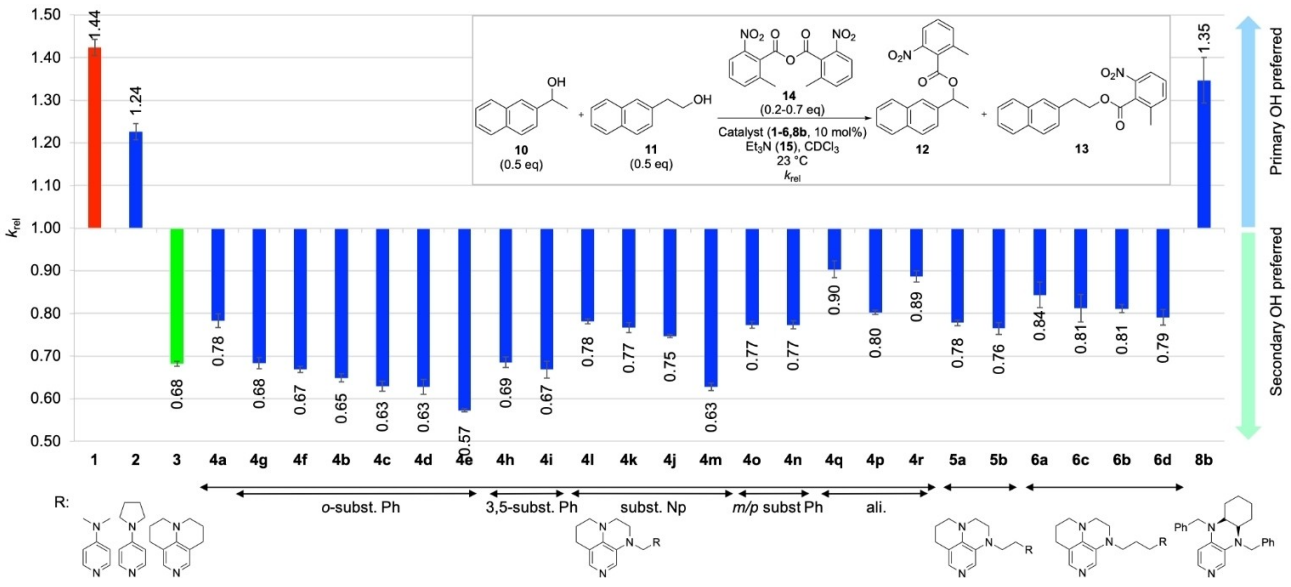

Figure 3. Relative rate constants k_{rel} for secondary alcohol **10** vs primary alcohol **11** with anhydride **14** catalysed by various catalysts **1**–**6**, **8b**.

Research Article
doi.org/10.1002/ejoc.202101521

selectivity values decrease slightly, the smallest value (and thus the highest preference for secondary alcohol **10**) being found for **4d** with $k_{rel} = 0.63$. Whether the *ortho*-substituent is attached through a CH_2-group (as in **4f**) or an ether oxygen bridge (as in **4g**) appears not to impact the obtained selectivities. The best result in this group with $k_{rel} = 0.57$ is obtained for **4e** carrying a 7-methoxynaphth-2-yl substituent. This selectivity value may reflect the size of the 2-naphthyl substituent as well as the electronic influence of the attached methoxy group. Moving the attached substituents to *meta* (as in **4n**) or *para* position (as in the dimethyl amino-substituted system **4o**) leads to selectivities closely similar to those obtained for **4a**. Slightly better selectivities are obtained for the 3,5-disubstituted systems **4h** with $k_{rel} = 0.69$ (where two *t*Bu units may act as electron donor and DED-groups)[23b] and **4i** with $k_{rel} = 0.67$ (where CF_3 groups act as electron withdrawing substitutents). Expanding the core side chain unit from Ph (as in **4a**) to naphthyl attached at C1 (as in **4j** and **4k**) or C2 (as in **4l**) shows no significant change in selectivity. Addition of a phenyl group at C1 position to this latter system as in **4m** leads to a small, but notable change in selectivity with $k_{rel} = 0.63$. Whether purely aliphatic side chains have systematically different effects as compared to aromatic side chains of equal carbon count was explored with **4q**, which can be seen as the hydrogenated complement to **4a**. Indeed, the selectivity is notably reduced now to $k_{rel} = 0.90$. Replacing the cyclohexyl by a *t*Bu substituent as in **4p** doesn't lead to a major change with $k_{rel} = 0.80$. In conclusion we can see that the 3,4-diaminopyridine variants explored in class I yield selectivity values closely similar to that of TCAP (**3**), where secondary alcohol **10** reacts approx. 1.5 times faster as compared to primary alcohol **11**. This selectivity can be rationalized assuming the previously reported "triple sandwich" acylation transition states,[21] where the 2-naphthyl side chain of alcohol **10** can form stronger non-covalent interactions with the catalyst pyridinium core unit as compared to alcohol **11**. If the catalyst surface is big enough (as is the case in the tricyclic pyridinium catalysts of type **3** and **4**), then the acylation of secondary alcohols is slightly preferred.

In Class II we find systems where the 3,4-diaminopyridine core unit is connected to the side chain with a slightly longer and thus more flexible C2 linker unit. However, comparing the results for **4a** (R=Ph, n = 1) and **5a** (R=Ph, n = 2) we see that both react with $k_{rel} = 0.78$. This is similarly true for the two catalysts carrying a naphth-1-yl side chain **4j** (n = 1) and **5b** (n = 2). We note in passing that reduction of linker flexibility as in catalyst **4r** leads to a notable reduction of selectivity. Increasing the linker length to n = 3 (class III) the acylation of secondary alcohol **10** is even less favored as can be seen for catalyst **6a** (R=Ph, n = 3) with $k_{rel} = 0.84$. For the larger naphth-1-yl side chain similar selectivities are obtained for all linker lengths with $k_{rel} = 0.75$ (**4j**, n = 1), $k_{rel} = 0.76$ (**5b**, n = 2) and $k_{rel} = 0.79$ (**6d**, n = 3). Further variation of the size of the substituent as in **6b** or **6c** also leads to no notable change in the selectivities, and we thus conclude that the length of the linker unit does NOT impact the catalytic behavior and the selectivity of the reaction. A lack of alignment of the attached aromatic substituents into one plane, which appears to impact acylation of secondary alcohol **10** more than that of primary alcohol **11** is determined for the tricyclic 3,4-diaminopyridine catalyst **8b** with $k_{rel} = 1.35$.

Absolute kinetics studies

Based on their performance in the 1:1 competition studies described above, seven catalysts were selected for further studies in the acylation of 1-(naphth-2-yl)ethane-1,2-diol **16** testing their ability to differentiate vicinal primary and secondary hydroxyl groups. Following earlier work on **16**[22] the initial formation of monoesters **17** and **18** and the subsequent second acylation to yield diester **19** were followed using absolute kinetics measurements (Scheme 3). Analysis of these results yields selectivity value $k_{rel,a}$ defined as the ratio between the effective acylation rate of primary hydroxyl group (k_3) and the secondary hydroxyl group of **16** (k_4). The ratio between the effective acylation rate of primary alcohol **18** (k_6) over the secondary alcohol **17** (k_5) is reflected in selectivity value $k_{rel,b}$ for the second acylation of the monoesters **17**/**18** to the diester **19**. The migration from **18** to **17** is neglected in this study.[22] With these definitions both selectivity values $k_{rel,a}$ and $k_{rel,b}$ reflect the acylation selectivities for primary over secondary hydroxyl groups. For **16** as a substrate we had found earlier that suitable catalyst/reagent combinations lead to an inversion of selectivity in favor of the secondary hydroxyl group.[22] As the acylation reagent we employ an excess (1.5 eq.) of 2-methyl-6-nitrobenzoic anhydride **14** in combination with 10 mol% of the corresponding Lewis base catalyst and Et_3N (2.0 eq.) as auxiliary base in $CDCl_3$ at +23 °C (for details see SI). The known catalysts DMAP (**1**), PPY (**2**), and TCAP (**3**) were again included as reference systems. The four 3,4-diaminopyridine catalysts tested in the acylation of diol **16** include the *ortho* substituted phenyl-

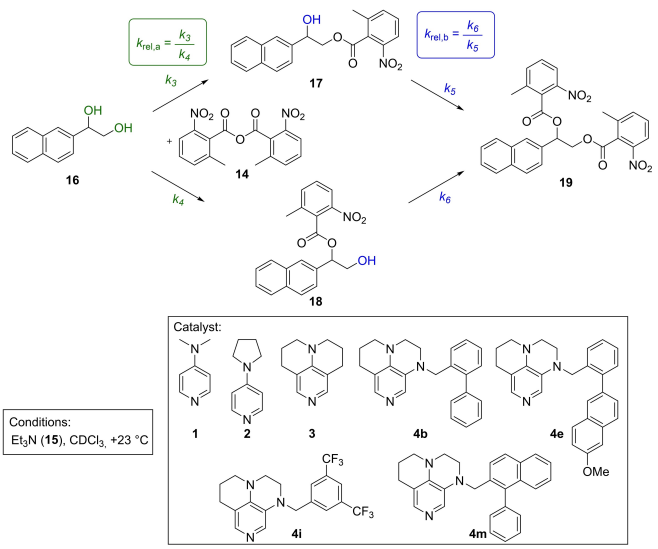

Scheme 3. Acylation of 1-(naphth-2-yl)ethane-1,2-diol **16** with 2-methyl-6-nitrobenzoic anhydride **14** mediated by catalysts **1**–**4** in the presence of Et_3N (**15**) at +23 °C.

Research Article
doi.org/10.1002/ejoc.202101521

based catalysts **4b,e**, the 3,5-disubstituted phenyl-based catalyst **4i**, and the *ortho*-substituted 2-naphthyl catalyst **4m**. Mole fractions for substrates **16**–**19** have been determined by ^{1}H NMR spectroscopy at various time intervals, and the effective rate constants k_3–k_6 have then been determined from these data by numerical kinetics simulations (see SI).[28] From the time dependence of the mole fraction of monoester **17** shown in Figure 4a we see that the effective rate constant k_3 for acylation of the primary hydroxyl group in **16** is largest for DMAP (**1**) and smallest for 3,4-diaminopyridine catalyst **4m**. It is particularly surprising that catalyst **1** is more reactive here than TCAP (**3**), which is in contrast to most other reactivity studies with these two Lewis bases.[6,12,29] Quantitative analysis in the framework of the mechanistic model shown in Scheme 3 yields the values shown in Table 1 and thus an approx. 10-fold reactivity difference between the fastest and slowest catalysts. A similar reactivity ordering is also found for acylation of the secondary hydroxyl group in **16** as is reflected in the time dependence of the mole fraction of monoester **18** shown in Figure 4b and the numerical values of rate constant k_4 in Table 1, except that **4i** is slightly more active than **1** in this case. A third measure of catalytic activity can be obtained from analysis of the time dependent conversion of all hydroxyl groups present in **16**–**18** as shown in Figure 4c, where again **4i** appears to be most active. The ratio of k_3 and k_4 and thus the primary/secondary selectivity of the first acylation step ($k_{rel,a}$ values in Table 1) is largest for DMAP (**1**) with $k_{rel,a} = 2.49$ and then approaches unity for the less active catalysts. This parallels the chemoselectivities presented in Figure 3, where **1** showed the largest preference for the acylation of primary alcohol **11** over secondary alcohol **10**. In contrast to these intermolecular competition experiments, TCAP (**3**) is not effective in inverting the primary/secondary selectivity in the acylation of diol **16** with $k_{rel,a} = 1.47$. The 3,4-diaminopyridine catalysts **4b,e,i** and **m** all show $k_{rel,a}$ values close to 1.0, the individual differences being too small for meaningful structure/ activity analyses. The acylation of monoesters **17** vs. **18** to diester **19** is systematically slower than the initial acylation step, and only for catalysts **1**–**3** and **4i** could full conversion to **19** be observed. For catalysts **4b,e** and **m** only conversions of up to 60% could be realized even at extended reaction times (for more details see SI). From the time-dependent decrease of the mole fraction of monoester **17** shown in Figure 4a we see that the effective rate constant k_5 for acylation of the secondary hydroxyl group in **17** is largest for 3,4-diaminopyridine catalyst **4i** and smallest for PPY (**2**). Quantitative analysis in the framework of the mechanistic model shown in Scheme 3 yields the values shown in Table 2 and thus an approx. 2.5-fold reactivity difference between the fastest and slowest catalysts. The acylation of the primary hydroxyl group in **18**, as described by the time dependent decrease of the mole fraction of monoester **18** shown in

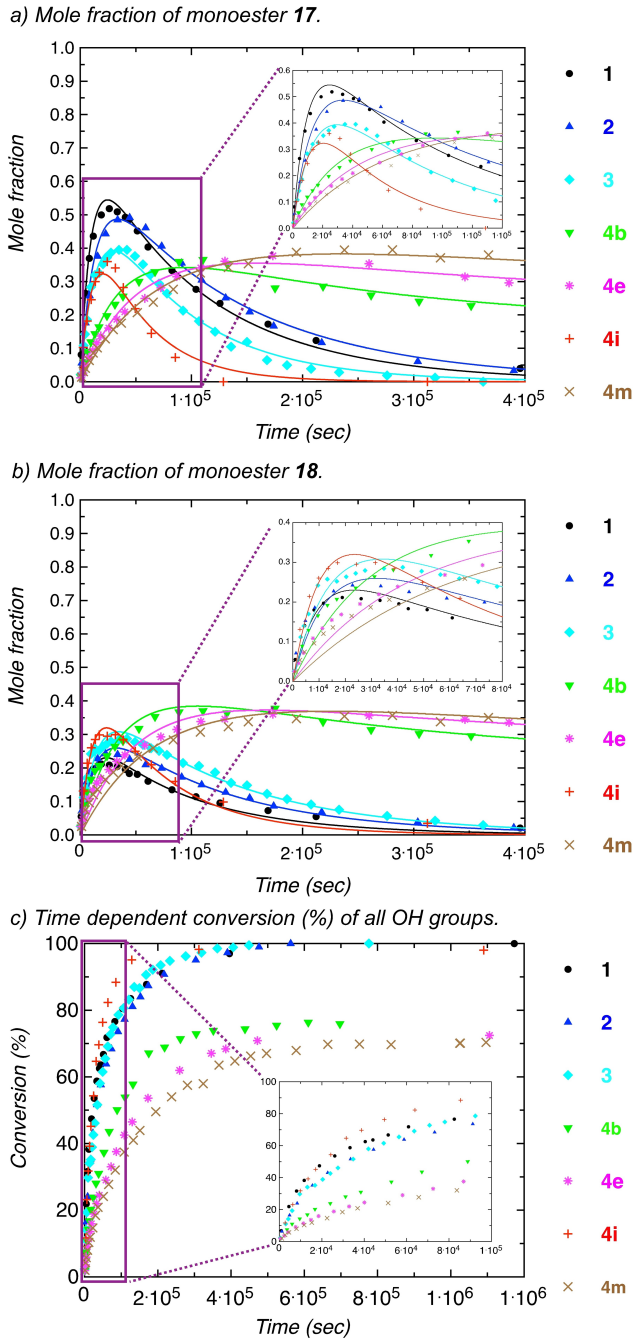

Figure 4. Time development (in sec) of a) the mole fraction of monester **17**, b) the mole fraction of monoester **18**, and c) the conversion all OH-groups (%) in the acylation of diol **16** with anhydride **14** mediated by catalysts **1**–**3**, **4b,e,i** and **m**.

Table 1. Effective rate constants k_3 and k_4 and the corresponding relative rate constant $k_{rel,a}$ for catalysts **1**–**3**, **4b,e,i** and **m** for the first acylation of polyol **16** determined through absolute kinetics. The relative rate constant k_{rel} for the acylation of alcohols **10** and **11** with **14** catalysed by **1**–**3**, **4b,e,i** and **m** has been determined through turnover-limited competition experiments.

Entry	Catalyst	k_3 (x10^{-3})[a,b]	k_4 (x10^{-3})[a,b]	$k_{rel,a}$[a]	k_{rel}[a]
1	**1**	69.9 ± 12.39	27.9 ± 2.99	2.49 ± 0.178	1.44 ± 0.016
2	**2**	38.7 ± 2.30	21.8 ± 1.85	1.78 ± 0.046	1.24 ± 0.017
3	**3**	36.6 ± 5.26	24.7 ± 2.35	1.47 ± 0.073	0.68 ± 0.006
4	**4i**	35.7 ± 0.04	32.1 ± 0.04	1.11 ± 0.003	0.67 ± 0.017
5	**4b**	9.2 ± 0.10	9.6 ± 1.29	0.97 ± 0.026	0.65 ± 0.009
6	**4m**	5.9 ± 0.84	5.8 ± 0.75	1.03 ± 0.011	0.63 ± 0.008
7	**4e**	6.7 ± 0.11	6.9 ± 0.08	0.98 ± 0.005	0.57 ± 0.003

[a] Averaged values (see SI). [b] In L mol^{-1} s^{-1}.

Table 2. Effective rate constants k_5 and k_6 and the corresponding relative rate constant $k_{rel,b}$ for catalysts **1**–**3** and **4i** for the second acylation of polyol **16** determined through absolute kinetics. The relative rate constant k_{rel} for the acylation of alcohols **10** and **11** with **14** catalysed by **1**–**3** and **4i** has been determined through turnover-limited competition experiments.

Entry	Catalyst	k_5 (x10^{-3})[a,b]	k_6 (x10^{-3})[a,b]	$k_{rel,b}$[a]	k_{rel}[a]
1	**4i**	18.2 ± 0.76	10.9 ± 2.21	0.59 ± 0.102	0.67 ± 0.017
2	**3**	14.6 ± 4.07	9.32 ± 2.34	0.64 ± 0.019	0.68 ± 0.006
3	**1**	10.3 ± 2.20	11.2 ± 2.00	1.10 ± 0.041	1.44 ± 0.016
4	**2**	6.9 ± 0.24	8.41 ± 0.80	1.21 ± 0.073	1.24 ± 0.017

[a] Averaged values (see SI). [b] In L mol^{-1} s^{-1}.

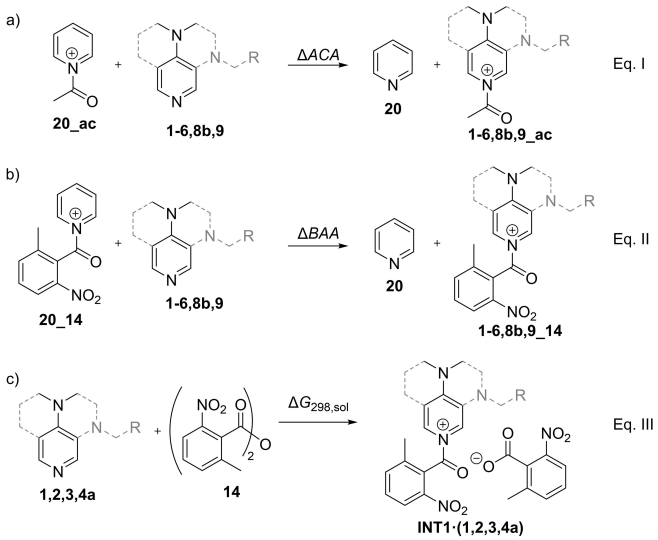

Scheme 4. Model of a) acetyl cation affinity number (Δ*ACA*, Eq. I), b) benzoic anhydride affinity number (Δ*BBA*, Eq. II) and c) Gibbs free reaction energy of the formation of **INT1** (Eq. III).

Table 3. Acetyl cation affinity numbers (Δ*ACA*), benzoic anhydride affinity numbers *(*Δ*BAA*), and free energy values for the formation of INT1 (in kJ mol^{-1}).

Entry	Catalyst	Δ*ACA*[a]	Δ*BAA*[a]	INT1[b]
1	**1**	−57.9	−58.4	+20.6
2	**2**	−63.1	−63.4	+12.5
3	**8b**	−71.1	−85.8	/
4	**4i**	−72.6	−91.4	/
5	**3**	−75.0	−76.9	+8.3
6	**4j**	−80.3	−83.7	/
7	**4a**	−81.5	−95.3	−2.7
8	**5a**	−81.6	−89.5	/
9	**5b**	−83.8	−88.5	/
10	**9**	−84.1	−99.9	/
11	**6a**	−85.2	−93.0	/
12	**4b**	−85.4	−101.2	/
13	**4m**	−87.8	−94.6	/
14	**6d**	−91.0	−93.1	/
15	**4e**	−93.6	−96.6	/

[a] ΔH_{298}(SMD(CHCl$_3$)/B3LYP-D3/6-31 + G(d)), in kJ mol^{-1}. [b] $\Delta G_{298,sol}$-(DLPNO-CCSD(T)/def2-TZVPP//SMD(CHCl$_3$)/B3LYP-D3/6-31 + G(d)), in kJ mol^{-1}.

Figure 4b and the numerical values of rate constant k_6 in Table 2, proceeds with similar efficiency with all catalysts. Again DMAP (**1**) has the largest effective rate constant k_6 and PPY (**2**) the smallest. The ratio of k_6 and k_5 and thus the primary/secondary selectivity of the second acylation step ($k_{rel,b}$ values in Table 2) is largest for PPY (**2**) with $k_{rel,b} = 1.21$ and inverted to the secondary hydroxyl group for tricyclic catalyst systems TCAP (**3**) with $k_{rel,b} = 0.64$ and **4i** with $k_{rel,b} = 0.59$.

Acetyl cation affinity values (ΔACA)

In how far intramolecular interactions between catalyst side chains and the *N*-aminopyridinium core unit influences the Lewis basicity of the catalysts was explored by the calculation of acetyl cation affinities (Δ*ACA*) at the SMD(CHCl$_3$)/B3LYP-D3/6-31 + G(d) level of theory.[30] As shown in Eq. I (Scheme 4a) these are defined as the reaction enthalpies ΔH_{298} for acetyl group transfer from acetylpyridinium cation **20_ac**.[12,14,29a,31] The Lewis basicity of 4-aminopyridine catalysts **1** and **2** is lower than that of 3,4-diaminopyridines and is in the range of $\Delta ACA = -57.9$ to -63.1 kJ mol^{-1} (Table 3, entries 1–2). Around 10 kJ mol^{-1} higher basicities are found for tricyclic catalysts **4i** (Δ*ACA* = -72.6 kJ mol^{-1}, entry 4) and **3** (Δ*ACA* = -75.0 kJ mol^{-1}, entry 5). Most of the catalysts **4, 5** and **6** have affinity values between Δ*ACA* = -80.3–93.6 kJ mol^{-1}, whereby **4e** with Δ*ACA* = -93.6 kJ mol^{-1} is the most Lewis-basic catalyst of this class (entry 15).[32] The tricyclic catalyst **8b** has a similar basicity as TCAP with Δ*ACA* = -71.1 kJ mol^{-1}, while the triaminopyridine catalyst **9** is of intermediate basicity with Δ*ACA* = -84.1 kJ mol^{-1}. The experimental studies described above employ 2-methyl-6-nitrobenzoic anhydride (**14**) as the electrophilic reagent, and additional benzoic anhydride affinities (Δ*BAA*) were therefore calculated for this system as defined by Eq. II (Scheme 4b and Table 3). The graphical presentation of Δ*ACA* and Δ*BAA* values in Figure 5 shows both affinity measures to follow similar trends, but also indicates that the Δ*BAA* values are slightly larger (more negative) for the tricyclic catalysts. Particularly larger changes in affinity are found for the benzyl-substituted catalysts **4a**, **4b**, and **4i**, as well as **8b** and **9**.

With the relative acetyl cation affinity (Δ*ACA*) values in hand, we can analyze the structural differences between the various acylated catalysts and thus test the hypothesis of stabilizing non-covalent interactions presented in Scheme 1. The most stable conformers of the acylpyridinium cations of selected catalysts are shown in Figure 6 together with critical distances between the acylpyridinium core units and the closest side chain atoms. In the (biphen-2-yl)methyl-substituted 3,4-diaminopyridine intermediates **4b_ac, 4e_ac**, and **4m_ac** we can indeed recognize the expected sandwich structures between side chain phenyl groups and the acylpyridinium core fragment with ring-to-ring distances of $r = 350$–377 pm typical for stacking conformations. The shortest distance of $r = 350$ pm can be found for the most Lewis basic catalyst **4e_ac**, where the side chain aryl group is positioned directly over the catalytically active nitrogen atom.[34] In contrast, no such interactions can be seen in the acylpyridinium intermediate of catalyst **4i** characterized by a comparatively low Δ*ACA* value. Whether alkyl group linkers of different lengths can be employed to steer the attached side chain π-systems into a

Research Article
doi.org/10.1002/ejoc.202101521

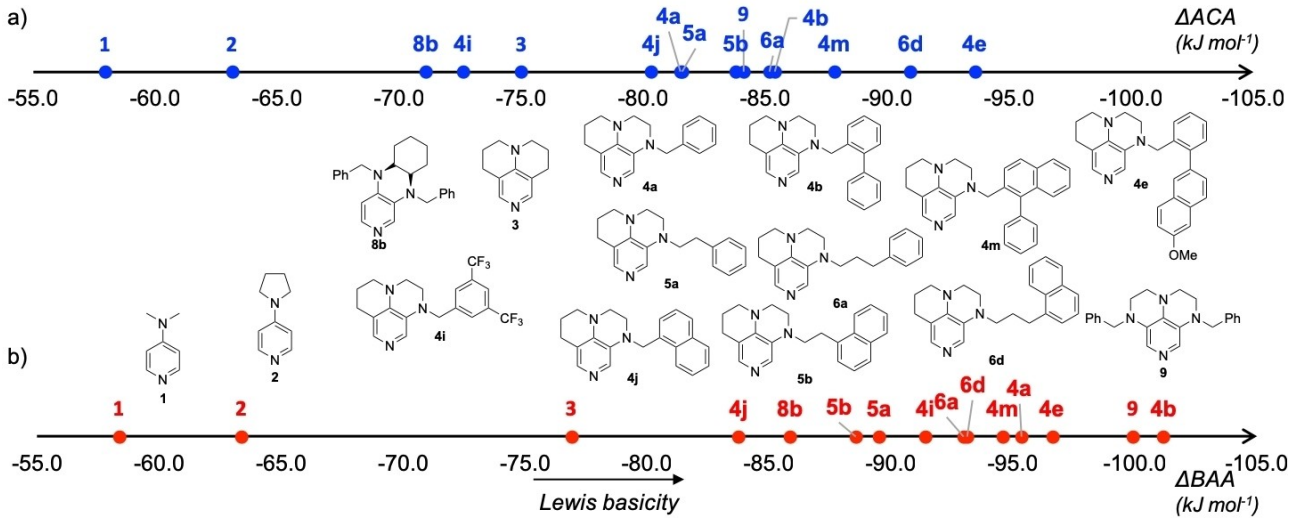

Figure 5. a) Acetyl cation affinity values (Δ*ACA, blue*), and b) benzoic anhydride affinity values (Δ*BAA, red*) for catalysts **1**–**6**, **8 b**, and **9**.

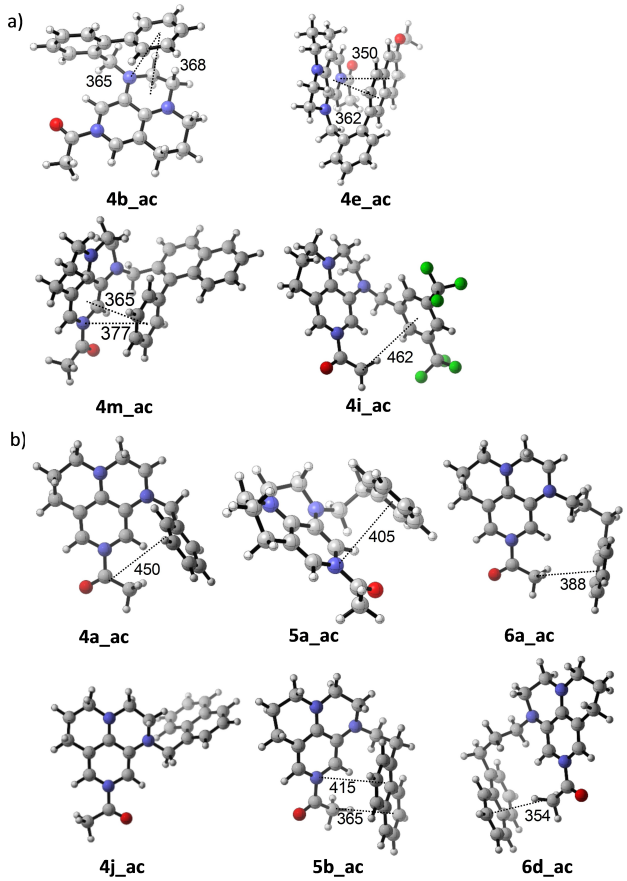

Figure 6. Geometries of acetyl cation adducts optimized at the SMD($CHCl_3$)/B3LYP-D3/6-31 + G(d) level of theory for a) catalysts **4 b**, **4 e**, **4 m** and **4 i**, and b) catalysts **4 a**,**j**, **5 a**,**b** and **6 a**,**d** together with selected distances (in pm) between side chains and the acetylpyridinium core unit.[33]

stacking orientation was tested for catalysts **4 a**, **5 a**, and **6 a** with linker lengths of n = 1–3. The best alignment between acylpyridinium core and side chain phenyl substituents could be seen in **5 a**, but even then, the distances between the two units was significantly larger at $r = 405$ pm as compared to that in **4 b_ac**. For the system with the largest linker length **6 a_ac** the dominant side chain/acylpyridinium core interaction appears to be a CH-π interaction between the attached π-system and the acetyl C–H bonds.[35] Effectively the same conclusions were obtained for the acylpyridinium intermediates of 1-naphthyl substituted catalysts **4 j**, **5 b**, and **6 d**, where again the linker length varies from n = 1–3 (Figure 6b).

In earlier studies it could be shown that cation affinity values of Lewis base catalysts correlate well with their effective rate constants towards electrophiles.[12,14,29a,31] Whether this is also the case for the first acylation of diol **16** studied here is shown in Figure 7. Plotting the Δ*ACA* values over the natural logarithm of effective rate constant ln k_3 (acylation of primary OH-group in **16**) a linear correlation of good fidelity is obtained (Figure 7, red triangles, $R^2 = 0.89$). It is, however, quite unexpected that catalysts with lower Lewis basicity such as **1** or **2** accelerate the acylation more strongly as compared to more potent Lewis base catalysts such as **3** or **4 b**,**e**,**m**. This finding (specifically for catalysts **1**–**3**) is in contrast to the findings of earlier studies on Lewis base-mediated acylation reactions.[6,12] The same type of correlation, but with a smaller slope, is also found for rate constant ln k_4 (acylation of secondary hydroxyl group in **16**, Figure 7b, green cycles, $R^2 = 0.73$). It is the difference in the slopes for the acylation of the primary and the secondary hydroxyl group in diol **16** that leads to a direct link between catalyst Lewis basicity and acylation regioselectivity as quantified by $k_{rel,a}$ in Table 1. In order to identify possible reasons for the comparatively low catalytic activity of the most Lewis basic catalysts studied here, we also calculated the full Gibbs free energy for the reaction of catalysts **1**–**4** with anhydride **14** to yield the full *N*-acylpyridinium ion pair intermediates **INT1** at the DLPNO-CCSD(T)/def2-TZVPP//SMD($CHCl_3$)/B3LYP-D3/6-31 + G(d) level of theory (Eq. III, Scheme 4).[30,36] Based on earlier theoretical studies we assume

Research Article
doi.org/10.1002/ejoc.202101521

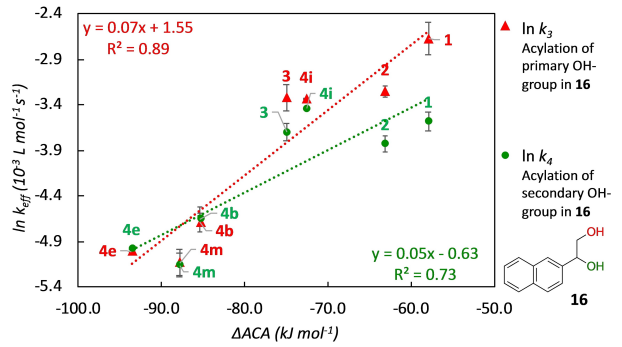

Figure 7. Plot of ΔACA (kJ mol^{-1}) vs. lnk_3 (red triangles) and lnk_4 (green circles) catalysed by **1**–**3**, **4b**,**e**,**i** and **m**.

that the formation of **INT1** is the first step of the catalytic cycle.[21] If **INT1** is too stable, the energy barrier for the subsequent alcohol acylation step could be negatively affected.[37] For DMAP a Gibbs free energy of $\Delta G_{298}(\mathbf{1}) = +20.6$ kJ mol^{-1} was obtained (Table 3). For increasingly Lewis basic catalysts these energies become more favorable with values of $\Delta G_{298}(\mathbf{2}) = +12.5$ kJ mol^{-1}, $\Delta G_{298}(\mathbf{3}) = +8.3$ kJ mol^{-1}, and $\Delta G_{298}(\mathbf{4a}) = -2.7$ kJ mol^{-1}. This last value thus implies that the equilibrium between free catalyst **4a** and its acylpyridinium ion pair intermediate **INT14a** may tip towards the latter as a function of absolute catalyst/reagent concentrations. As shown in Figure 8, the various measures of Lewis basicity studied here (ΔACA(**x**), ΔBAA(**x**) a ΔG_{298}(**x**)) are well correlated.

Together with the direct ^{1}H NMR-spectroscopic detection of **INT1** for the catalysts **1**, **3**, and **4a** (see SI for further details) we thus assume that the stabilities of acylpyridinium intermediates formed with anhydride **14** are, at least in part, responsible for the inverse correlation of acylation rate and Lewis basicity. In addition, we note that hydrogen bonding interactions between the two hydroxyl substituents in diol **16** moderated its reactivity.

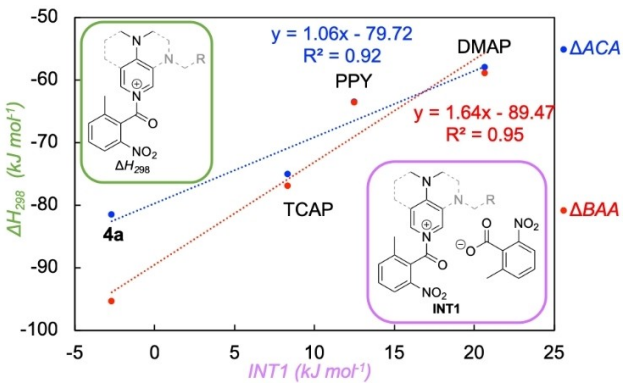

Figure 8. Plot of the stability of **INT1** (ΔG_{298} in kJ mol^{-1}) vs. ΔACA (ΔH_{298} in kJ mol^{-1}) for Lewis base catalysts **1**–**3** and **4a**.

Conclusion

A group of 24 tricyclic pyridine-based Lewis base catalysts have been synthesized with the goal of performing selective acylation reactions of secondary hydroxyl groups in aromatic 1,2-ethanediols with 2-methyl-6-nitrobenzoic anhydride. The acylation of secondary instead of primary hydroxyl groups depends on the surface of the Lewis base and its steric demand. The formation of sandwich structures between DED-substituents of Lewis base catalysts and the tricyclic pyridinium core units increases the Lewis basicity by stabilization of acylpyridinium cations and supports the acylation of secondary alcohols in separated ethanol systems as well as in 1,2-diols. Somewhat surprisingly, the positioning of DED-substituents is less effective through flexible CH_2-linker units as compared to *ortho*-substituted aryl units. Some of the highly Lewis basic pyridine-based catalysts studied here form comparatively stable *N*-acylpyridinium cation intermediates detected both by experimental and quantum chemical analysis. This stability may actually impede catalytic turnover in acylation reactions. In contrast, catalyst **4i** containing two CF_3 groups is predicted to be a more active and selective organocatalyst than **1**. The second finding of this study is that in 1,2-diol systems the acylation is quite fast with less nucleophilic and sterically demanding catalysts. Tests towards the use of the reagent/catalyst combinations explored here in reactions of polyol natural products are currently under way in our laboratories.

Experimental Section

Competition experiments: Three different $CDCl_3$ stock solutions were prepared under nitrogen. Stock solution A contained the secondary alcohol **10** and primary alcohol **11** each at a concentration of 0.05 M. Stock solution B contained anhydride **14** (0.1 M), while stock solution C contained 0.15 M Et_3N and catalyst **1**–**8** at a concentration of 0.01 M. Stock solution B was diluted in four discrete steps. The concentrations of the new solutions were fixed at 20, 35, 50, and 70% of the initial stock solution B. Under nitrogen 0.4 mL of stock solution A, 0.4 mL of stock solution C, and 0.4 mL of stock solution B1-4 were transferred to a GC vial by using a Hamilton syringe. The GC vial was then capped under nitrogen and placed in the GC vial holder with stirring. The competition experiments were considered finished when the reaction with the highest anhydride concentration (GC vial 4) was complete. The reaction was monitored by ^{1}H NMR spectroscopy.

Kinetics studies: Three different $CDCl_3$ stock solutions containing 0.02 M 1,2-diol **16** (A), 0.06 M acid anhydride **14** (B), and a combination of 0.08 M Et_3N and 0.004 M **1**–**8** (C) were prepared under nitrogen. The reaction was analysed by ^{1}H NMR as recorded on a Bruker Avance III 400 machine. NMR tubes were first dried under vacuum using a special home-made apparatus and flushed with nitrogen, and 0.2 mL of stock solution A, 0.2 mL of stock solution C and 0.2 mL of stock solution B were then transferred under nitrogen to the NMR tube by use of a Hamilton syringe. After closing the NMR tube, the reaction mixture was shaken and introduced into the NMR machine.

Computational details: All geometry optimizations and vibrational frequency calculations have been performed using the B3LYP-D3 hybrid functional[30c–e] in combination with the 6-31+G(d) basis

set.[38] Solvent effects for chloroform have been taken into account with the SMD continuum solvation model.[30b] This combination has recently been found to perform well for Lewis base-catalysed reactions.[39] Thermochemical corrections to 298.15 K have been calculated for all stationary points from unscaled vibrational frequencies obtained at this same level. Solvation energies have been obtained as the difference between the energies computed at B3LYP-D3/6-31+G(d) in solution and in gas phase. For the elucidation of the mechanism, the thermochemical corrections of optimized structures have been combined with single point energies calculated at the DLPNO-CCSD(T)/def2-TZVPP//B3LYP-D3/6-31+G(d) level.[36,40] Solvation energies have been added to the energies computed at DLPNO-CCSD(T)/def2-TZVPP//SMD($CHCl_3$)/B3LYP-D3/6-31+G(d) level to yield free energies G_{298} at 298.15 K. Free energies in solution have been corrected to a reference state of 1 mol/L at 298.15 K through addition of RTln(24.46) = +7.925 kJ/mol to the free energies. All calculations have been performed with Gaussian 09[41] and ORCA version 4.0.[42] Conformation search was performed with Maestro.[43]

Crystallographic data: Deposition numbers 2110005 (for **25c**), 2110006 (**27c**), and (2110007 for (**4p**) contain the supplementary crystallographic data for this paper. These data are provided free of charge by the joint Cambridge Crystallographic Data Centre and Fachinformationszentrum Karlsruhe Access Structures service www.ccdc.cam.ac.uk/structures.

Acknowledgements

This work was financially supported by the Deutsche Forschungsgemeinschaft (DFG) through the Priority Program "Control of London Dispersion Interactions in Molecular Chemistry" (SPP 1807), grant ZI 436/17-1. Open Access funding enabled and organized by Projekt DEAL.

Conflict of Interest

The authors declare no conflict of interest.

Data Availability Statement

The data that support the findings of this study are available in the supplementary material of this article.

Keywords: Acylation · Anhydrides · Lewis bases · Noncovalent interactions · Regioselectivity

[1] a) O. Robles, D. Romo, *Nat. Prod. Rep.* **2014**, *31*, 318–334; b) K. C. Nicolaou, J. S. Chen, *Classics in Total Synthesis III*, Wiley-VCH, Weinheim, **2011**.
[2] a) P. S. Baran, T. J. Maimone, J. M. Richter, *Nature* **2007**, *446*, 404–408; b) G. Zong, E. Barber, H. Aljewari, J. Zhou, Z. Hu, Y. Du, W. Q. Shi, *J. Org. Chem.* **2015**, *80*, 9279–9291; c) M. Koshimizu, M. Nagatomo, M. Inoue, *Angew. Chem. Int. Ed.* **2016**, *55*, 2493–2497; *Angew. Chem.* **2016**, *128*, 2539–2543.
[3] S. M. Polyakova, A. V. Nizovtsev, R. A. Kunetskiy, N. V. Bovin, *Russ. Chem. Bull.* **2015**, *64*, 973–989.
[4] a) C. A. Lewis, S. J. Miller, *Angew. Chem. Int. Ed.* **2006**, *45*, 5616–5619; *Angew. Chem.* **2006**, *118*, 5744–5747; b) S. Araki, S. Kambe, K. Kameda, T. Hirashita, *Synthesis* **2003**, *2003*, 0751–0754; c) P. G. M. Wuts, *Greene's Protective Groups in Organic Synthesis*, 5 ed., John Wiley & Sons, Hoboken, New Jersey, **2014**; d) A. Baldessari, C. P. Mangone, E. G. Gros, *Helv. Chim. Acta* **1998**, *81*, 2407–2413; e) K. Ishihara, H. Kurihara, H. Yamamoto, *J. Org. Chem.* **1993**, *58*, 3791–3793; f) T. Maki, F. Iwasaki, Y. Matsumura, *Tetrahedron Lett.* **1998**, *39*, 5601–5604; g) F. Iwasaki, T. Maki, W. Nakashima, O. Onomura, Y. Matsumura, *Org. Lett.* **1999**, *1*, 969–972; h) J. E. Taylor, J. M. J. Williams, S. D. Bull, *Tetrahedron Lett.* **2012**, *53*, 4074–4076.
[5] a) P. Peng, M. Linseis, R. F. Winter, R. R. Schmidt, *J. Am. Chem. Soc.* **2016**, *138*, 6002–6009; b) M. Nahmany, A. Melman, *Org. Biomol. Chem.* **2004**, *2*, 1563–1572; c) N. A. Afagh, A. K. Yudin, *Angew. Chem. Int. Ed.* **2010**, *49*, 262–310; *Angew. Chem.* **2010**, *122*, 270–320; d) A. H. Haines, *Adv. Carbohydr. Chem. Biochem.* **1976**, *33*, 11–109; e) S. E. Denmark, G. L. Beutner, *Angew. Chem. Int. Ed.* **2008**, *47*, 1560–1638; *Angew. Chem.* **2008**, *120*, 1584–1663; f) A. C. Spivey, S. Arseniyadis, *Angew. Chem. Int. Ed.* **2004**, *43*, 5436–5441; *Angew. Chem.* **2004**, *116*, 5552–5557.
[6] a) E. S. Munday, M. A. Grove, T. Feoktistova, A. C. Brueckner, D. M. Walden, C. M. Young, A. M. Z. Slawin, A. D. Campbell, P. H.-Y. Cheong, A. D. Smith, *Angew. Chem. Int. Ed.* **2020**, *59*, 7897–7905; *Angew. Chem.* **2020**, *132*, 7971–7979; b) A. Kinens, S. Balkaitis, O. K. Ahmad, D. W. Piotrowski, E. Suna, *J. Org. Chem.* **2021**, *86*, 7189–7202.
[7] a) C. E. Müller, P. R. Schreiner, *Angew. Chem. Int. Ed.* **2011**, *50*, 6012–6042; *Angew. Chem.* **2011**, *123*, 6136–6167; b) E. Vedejs, S. T. Diver, *J. Am. Chem. Soc.* **1993**, *115*, 3358–3359; c) E. Vedejs, N. S. Bennett, L. M. Conn, S. T. Diver, M. Gingras, S. Lin, P. A. Oliver, M. J. Peterson, *J. Org. Chem.* **1993**, *58*, 7286–7288; d) E. Vedejs, O. Daugulis, S. T. Diver, *J. Org. Chem.* **1996**, *J. Org. Chem.* **1993**, 58, 7286–7288;61, 430–431; e) V. B. Birman, X. Li, Z. Han, *Org. Lett.* **2007**, *9*, 37–40; f) S. J. Miller, G. T. Copeland, N. Papioannou, T. E. Hortsmann, E. M. Ruehl, *J. Am. Chem. Soc.* **1998**, *120*, 1629–1630.
[8] L. M. Litvinenko, A. I. Kirichenko, *Dokl. Akad. Nauk. SSSR Ser. Khim.* **1967**, *176*, 97–100.
[9] a) G. Höfle, W. Steglich, H. Vorbrüggen, *Angew. Chem. Int. Ed.* **1978**, *17*, 569–583; *Angew. Chem.* **1978**, *90*, 602–615; b) W. Steglich, G. Höfle, *Angew. Chem. Int. Ed.* **1969**, *8*, 981–981; *Angew. Chem.* **1969**, *81*, 1001–1001.
[10] a) W. Steglich, G. Höfle, *Tetrahedron Lett.* **1970**, *11*, 4727–4730; b) A. Hassner, L. R. Krepski, V. Alexanian, *Tetrahedron* **1978**, *34*, 2069–2076.
[11] M. R. Heinrich, H. S. Klisa, H. Mayr, W. Steglich, H. Zipse, *Angew. Chem. Int. Ed.* **2003**, *42*, 4826–4828; *Angew. Chem.* **2003**, *115*, 4975–4977.
[12] R. Tandon, T. Unzner, T. A. Nigst, N. De Rycke, P. Mayer, B. Wendt, O. R. P. David, H. Zipse, *Chem. Eur. J.* **2013**, *19*, 6435–6442.
[13] T. Kawabata, M. Nagato, K. Takasu, K. Fuji, *J. Am. Chem. Soc.* **1997**, *119*, 3169–3170.
[14] Y. Wei, I. Held, H. Zipse, *Org. Biomol. Chem.* **2006**, *4*, 4223–4230.
[15] R. Tandon, T. A. Nigst, H. Zipse, *Eur. J. Org. Chem.* **2013**, *2013*, 5423–5430.
[16] S. Singh, G. Das, O. V. Singh, H. Han, *Org. Lett.* **2007**, *9*, 401–404.
[17] I. Held, S. Xu, H. Zipse, *Synthesis* **2007**, *2007*, 1185–1196.
[18] S. Yamada, *Chem. Rev.* **2018**, *118*, 11353–11432.
[19] T. Kawabata, W. Muramatsu, T. Nishio, T. Shibata, H. Schedel, *J. Am. Chem. Soc.* **2007**, *129*, 12890–12895.
[20] E. Kattnig, M. Albert, *Org. Lett.* **2004**, *6*, 945–948.
[21] S. Mayr, M. Marin-Luna, H. Zipse, *J. Org. Chem.* **2021**, *86*, 3456–3489.
[22] S. Mayr, H. Zipse, *Chem. Eur. J.* **2021**, *27*, 18084–18092.
[23] a) B. Pölloth, M. P. Sibi, H. Zipse, *Angew. Chem. Int. Ed.* **2021**, *60*, 774–778; *Angew. Chem.* **2021**, *133*, 786–791; b) J. P. Wagner, P. R. Schreiner, *Angew. Chem. Int. Ed.* **2015**, *54*, 12274–12296; *Angew. Chem.* **2015**, *127*, 12446–12471.
[24] The strong Lewis base catalyst **9** was not explored in the experimental part of this work. The reported X-ray structure demonstrates that the Ph rings are orientated such that intra- and intermolecular cation-π stacking interactions are not possible.
[25] J. Helberg, M. Marin-Luna, H. Zipse, *Synthesis* **2017**, *49*, 3460–3470.
[26] H. B. Kagan, J. C. Fiaud, *Top. Stereochem.* **1988**, *18*, 249–330.
[27] E. Larionov, F. Achrainer, J. Humin, H. Zipse, *ChemCatChem* **2012**, *4*, 559–566.
[28] S. Hoops, S. Sahle, R. Gauges, C. Lee, J. Pahle, N. Simus, M. Singhal, L. Xu, P. Mendes, U. Kummer, *Bioinformatics* **2006**, *22*, 3067–3074.
[29] a) J. Helberg, T. Ampßler, H. Zipse, *J. Org. Chem.* **2020**, *85*, 5390–5402; b) P. Patschinski, C. Zhang, H. Zipse, *J. Org. Chem.* **2014**, *79*, 8348–8357; c) V. Barbier, F. Couty, O. R. P. David, *Eur. J. Org. Chem.* **2015**, *2015*, 3679–3688; d) T. Tsutsumi, A. Saitoh, T. Kasai, M. Chu, S. Karanjit, A. Nakayama, K. Namba, *Tetrahedron Lett.* **2020**, *61*, 152047.

[30] a) S. Y. Park, J.-W. Lee, C. E. Song, *Nat. Commun.* **2015**, *6*, 7512; b) A. V. Marenich, C. J. Cramer, D. G. Truhlar, *J. Phys. Chem. B* **2009**, *113*, 6378–6396; c) S. Grimme, *J. Chem. Phys.* **2006**, *124*, 034108; d) A. D. Becke, *J. Chem. Phys.* **1993**, *98*, 5648–5652; e) C. Lee, W. Yang, R. G. Parr, *Phys. Rev. B* **1988**, *37*, 785–789.
[31] a) C. Lindner, R. Tandon, B. Maryasin, E. Larionov, H. Zipse, *Beilstein J. Org. Chem.* **2012**, *8*, 1406–1442; b) I. Held, E. Larionov, C. Bozler, F. Wagner, H. Zipse, *Synthesis* **2009**, *2009*, 2267–2277; c) Y. Wei, T. Singer, H. Mayr, G. N. Sastry, H. Zipse, *J. Comput. Chem.* **2008**, *29*, 291–297; d) Y. Wei, G. N. Sastry, H. Zipse, *J. Am. Chem. Soc.* **2008**, *130*, 3473–3477; e) I. Held, A. Villinger, H. Zipse, *Synthesis* **2005**, *2005*, 1425–1430.
[32] Here only a selection of calculated cationic affinity numbers is presented. A full analysis of the ΔACA values with all catalysts is shown in the SI.
[33] CYLVIEW: CYLview,1.0b; Legault, C. Y., Université de Sherbrooke, **2009** (http://www.cylview.org); 3D-Pictures were generated with the CYLview program.
[34] a) C. R. Kennedy, S. Lin, E. N. Jacobsen, *Angew. Chem. Int. Ed.* **2016**, *55*, 12596–12624; *Angew. Chem.* **2016**, *128*, 12784–12814; b) J. P. Gallivan, D. A. Dougherty, *J. Am. Chem. Soc.* **2000**, *122*, 870–874.
[35] O. Takahashi, Y. Kohno, M. Nishio, *Chem. Rev.* **2010**, *110*, 6049–6076.
[36] a) C. Riplinger, B. Sandhoefer, A. Hansen, F. Neese, *J. Chem. Phys.* **2013**, *139*, 134101; b) C. Riplinger, F. Neese, *J. Chem. Phys.* **2013**, *138*, 034106; c) F. Weigend, R. Ahlrichs, *Phys. Chem. Chem. Phys.* **2005**, *7*, 3297–3305.
[37] F. A. Carey, R. J. Sundberg, *Advanced Organic Chemistry Part A: Structure and Mechanisms*, 5 ed., Springer Science + Business Media, New York, **2007**.
[38] G. W. Spitznagel, T. Clark, J. Chandrasekhar, P. V. R. Schleyer, *J. Comput. Chem.* **1982**, *3*, 363–371.
[39] a) M. Marin-Luna, P. Patschinski, H. Zipse, *Chem. Eur. J.* **2018**, *24*, 15052–15058; b) M. Marin-Luna, B. Pölloth, F. Zott, H. Zipse, *Chem. Sci.* **2018**, *9*, 6509–6515.
[40] L. A. Curtiss, P. C. Redfern, K. Raghavachari, V. Rassolov, J. A. Pople, *J. Chem. Phys.* **1999**, *110*, 4703–4709.
[41] Gaussion 09, R. D.01, M. J. Frisch, G. W. Trucks, H. B. Schlegel, G. E. Scuseria, M. A. Robb, J. R. Cheeseman, G. Scalmani, V. Barone, B. Mennucci, G. A. Petersson, H. Nakatsuji, M. Caricato, X. Li, H. P. Hratchian, A. F. Izmaylov, J. Bloino, G. Zheng, J. L. Sonnenberg, M. Hada, M. Ehara, K. Toyota, R. Fukuda, J. Hasegawa, M. Ishida, T. Nakajima, Y. Honda, O. Kitao, H. Nakai, T. Vreven, J. A. Montgomery Jr., J. E. Peralta, F. Ogliaro, M. Bearpark, J. J. Heyd, E. Brothers, K. N. Kudin, V. N. Staroverov, R. Kobayashi, J. Normand, K. Raghavachari, A. Rendell, J. C. Burant, S. S. Iyengar, J. Tomasi, M. Cossi, N. Rega, J. M. Millam, M. Klene, J. E. Knox, J. B. Cross, V. Bakken, C. Adamo, J. Jaramillo, R. Gomperts, R. E. Stratmann, O. Yazyev, A. J. Austin, R. Cammi, C. Pomelli, J. W. Ochterski, R. L. Martin, K. Morokuma, V. G. Zakrzewski, G. A. Voth, P. Salvador, J. J. Dannenberg, S. Dapprich, A. D. Daniels, Ö. Farkas, J. B. Foresman, J. V. Ortiz, J. Cioslowski, D. J. Fox, Gaussian, Inc., W. CT, **2010**.
[42] F. Neese, *Wiley Interdiscip. Rev.: Comput. Mol. Sci.* **2012**, *2*, 73–78.
[43] Schrödinger Release 2019–2: Jaguar, Schrödinger, LLC, New York, NY, **2019**.

Manuscript received: December 16, 2021
Revised manuscript received: February 16, 2022
Accepted manuscript online: February 17, 2022